Performance and Application of a New Planar Array Infrared Spectrograph Operating in the Mid-Infrared (2000–975 cm^{-1}) Fingerprint Region

CHRISTIAN PELLERIN, CHRISTOPHER M. SNIVELY, D. BRUCE CHASE, and JOHN F. RABOLT*

Department of Materials Science and Engineering (C.P., C.M.S., J.F.R.), and Department of Chemical Engineering (C.M.S.), University of Delaware, Newark, Delaware 19716-3106; and DuPont Experimental Station, DuPont Inc., Wilmington, Delaware 19880 (D.B.C.)

A no-moving-part planar array infrared spectrograph (PA-IR) equipped with a 256 × 256 mercury cadmium telluride (MCT) focal plane array has been designed and constructed. The performance of the instrument, whose frequency range extends from 2000–975 cm^{-1}, has been assessed in terms of resolution, bandwidth, and signal-to-noise ratio. The PA-IR spectrograph is able to record spectra with an 8.7 ms time resolution and has peak-to-peak noise levels as low as 2.4 × 10^{-4} A.U. As a demonstration of the potential of PA-IR, the dynamics of reorientation of a liquid crystalline sample exposed to a single electric field pulse has been studied. It was shown that PA-IR can be used for the simultaneous acquisition of two orthogonally polarized spectra. The advantages and limitations of PA-IR, step-scan Fourier transform infrared (FT-IR), and ultra-rapid-scanning FT-IR for real-time studies of reversible and irreversible phenomena are thoroughly discussed.

Index Headings: **Planar array infrared spectrograph; Liquid crystal; Time-resolved spectroscopy.**

INTRODUCTION

In the last few decades, infrared spectroscopy and Fourier transform infrared (FT-IR) spectroscopy have become almost synonymous. FT-IR has virtually eliminated dispersive instruments from laboratories because of its multiplex advantage that allows the rapid recording of complete spectra, its frequency precision, and its high throughput. These advantages provide the sensitivity and signal-to-noise ratio necessary for the characterization of monolayers and allow the use of poorly transmitting accessories.[1] However, a limitation of FT-IR spectroscopy is the requirement of a fine control of the alignment of the optical components, which has restricted its use for field applications where mechanical vibrations or temperature instabilities are present. The time resolution of conventional FT-IR spectrometers is also limited by the necessity to accelerate and decelerate the moving mirror for each scan.[2]

Various approaches have been developed to increase the acquisition rate and time resolution for infrared measurements. In step-scan FT-IR, the moving mirror is stopped at a series of discrete positions and data are recorded as a function of time.[3–5] Combining the data from all steps generates a series of time-resolved interferograms with a time resolution that can be in the nanosecond range. The technique is, however, limited to phenomena that can be precisely reproduced hundreds of times during the course of the experiment. Asynchronous FT-IR sampling, in which the applied sample perturbation is not in phase with the data acquisition during a slow continuous scan, has also been used to study highly repeatable events with a μs time resolution.[6,7] Pump-probe techniques have also been used to follow the time evolution of repeatable phenomena, often photochemical reactions, with time resolutions in the ps and even the fs range.[8–10]

Nevertheless, these techniques are of little utility for the study of non-repeatable phenomena such as the macroscopic deformation of polymers, gas diffusion, etc. Even for repeatable events, one must be confident not only that the perturbation is perfectly reproducible but also that the initial state of the sample does not change with time and that no instrumental drift occurs during the long-term experiments. For example, in the study of the reorientation of liquid crystals under an applied electric field, one must ensure that the relaxation period is long enough for the sample to return to its initial state.

In this context, it is of great interest to develop techniques that allow the real-time study of irreversible phenomena and that of reversible phenomena in a shorter experimental time. State-of-the-art fast-scanning FT-IR spectrometers allow the acquisition of 8 cm^{-1} resolution spectra at a 60 Hz scan rate. Recently, an ultra-rapid-scanning FT-IR (URS-FT-IR) spectrometer using a rotating wedged disk mirror in place of the moving mirror was constructed by Griffiths et al.[2] and applied to the time-resolved study of irreversible polymer deformation.[11] This instrument allows scanning rates of 200 Hz
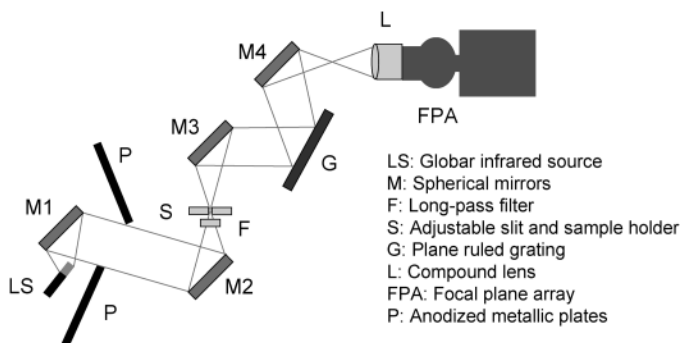
FIG. 1. Schematic representation of the planar array infrared spectrograph.

Legend for Fig. 1:
LS: Globar infrared source
M: Spherical mirrors
F: Long-pass filter
S: Adjustable slit and sample holder
G: Plane ruled grating
L: Compound lens
FPA: Focal plane array
P: Anodized metallic plates

with a 6 cm^{-1} resolution and has the potential for operation at 1000 Hz given the proper electronics.

In recent years, linear and two-dimensional focal plane arrays (FPA) have become commercially available and widely used for imaging purposes in combination with rapid[12] or step-scan FT-IR.[13–15] Such arrays have also been used to improve the time resolution of infrared spectroscopy. The combination of linear arrays with the asynchronous sampling technique has decreased the measurement time by measuring simultaneously 16 data points at different delays with respect to the sample perturbation.[16] Others have used linear arrays in a spectrographic approach. Richardson et al. dispersed the infrared light onto a 32-element InSb FPA using a monochromator, and then recorded spectra every 16 μs over a spectral coverage of 250 cm^{-1} at a resolution of 32 cm^{-1}.[17] Elmore et al. have recently reported the design of a no-moving-part planar array infrared spectrograph (PA-IR) based on a dispersive infrared spectrograph that contained a 320 × 256 InSb FPA detector.[18] The use of a large FPA detector eliminates the need for the exit slit present in classic dispersive spectrometers and thus provides a true multichannel advantage without the use of an interferometer. This instrument has allowed measurements in the 3400–2000 cm^{-1} region at a repetition rate of 60 Hz, and with a peak-to-peak noise level as low as 1.5 × 10^{-5} A.U.

In this work, we will describe the design of a new PA-IR spectrograph working in the fingerprint region of the mid-infrared (2000–975 cm^{-1}). Its performance will be assessed in terms of spectral range, resolution, and noise level. The possibility of multiple beam experiments will also be illustrated. Finally, the potential of PA-IR as a tool for real-time studies will be demonstrated by following the time-resolved reorientation of a liquid crystalline sample under an applied electric field. The advantages and limitations of this technique for time-resolved studies will be discussed.

EXPERIMENTAL

Planar Array Infrared Spectrograph. A schematic diagram of the PA-IR spectrograph is shown in Fig. 1. The instrument was built on an optical table. The light from a 1-cm-high broadband infrared source (LS) (Surfaceigniter Corporation, Chagrin Falls, OH) powered at 4.5 A and 24 V was collected and collimated by a spherical mirror (M1, 8 cm diameter, 15 cm focal length). A second identical mirror (M2) focused the beam on an

adjustable entrance slit (S, SPEX, Edison, NJ) and through the sample. It is also possible to introduce the sample holder in the collimated beam between M1 and M2. The infrared beam was then collimated by another matched spherical mirror (M3) and usually projected on a plane ruled diffraction grating (G) with 50 grooves/mm (SPEX, Edison, NJ), except when noted in the text. In order to reject the second and higher diffraction orders from the grating, a long-pass optical filter (F) with a cutoff of either 5 or 7.5 μm was used. The diffracted infrared light was finally collected and focused onto the focal plane of the detector (FPA) by a fourth spherical mirror (M4) and a STRIX 50 mm compound lens (L, Janos Technology, Townshend, VT). For the liquid crystal reorientation experiments, two stacked KRS-5 wire-grid polarizers were introduced between M1 and M2 to transmit parallel (*p*) and perpendicular (*s*) polarized light in the top and bottom portions of the spectral image, respectively.

The detector utilized was a liquid nitrogen-cooled 256 × 256 MCT focal plane array with 40 × 40 μm pixels (Santa Barbara Focalplane, Goleta, CA) equipped with two 14-bit analog-to-digital converters. The frame rate and integration time of the snapshot mode FPA were set to 115 (114.89) Hz and 71 μs, respectively. The linearity of the FPA was confirmed using a series of neutral density filters with a direct illumination of the FPA. A two-point non-uniformity correction was nevertheless performed using an anodized metal plate at ~20 and ~40 °C before data acquisition in order to compensate for bad pixels present in the FPA.

Planar Array Infrared Spectra. The raw single beam images were obtained using WinIR 3.6.0.4 (Santa Barbara Focalplane, Goleta, CA) and subsequently processed with home-written programs in MatLab 5.3 (MathWorks, Natick, MA). In addition to sample and background (open path) images, a dark background image was recorded with the optical path blocked by a room-temperature anodized metal plate in order to compensate for the thermal contribution of the environment to the FPA response and for potential stray light reaching the detector. For every pixel, the absorbance was calculated as:

$$A = -\log_{10}\left(\frac{I_s - I_{dbk}}{I_{bk} - I_{dbk}}\right) \quad (1)$$

where I_s, I_{bk}, and I_{dbk} are the single beam intensities recorded for the sample, background, and dark background, respectively.

For each series of PA-IR experiments, a reference spectral image of a 50 μm thick polystyrene (PS) film was recorded and used to compensate for the curvature observed in the images (see Fig. 2a) and to convert the pixel numbers into a wavenumber scale. The peak position of at least five PS bands was determined in both PA-IR and FT-IR spectra using GRAMS/AI 7.00 (Thermo Galactic, Salem, NH). The built-in solver of Excel (Microsoft, Redmond, WA) was then used to determine a third-order polynomial calibration function for converting the pixel numbers to wavenumbers.

For the noise level study, two open beam spectra of a given number of frames were recorded in sequence and the absorbance spectrum was calculated using Eq. 1 The
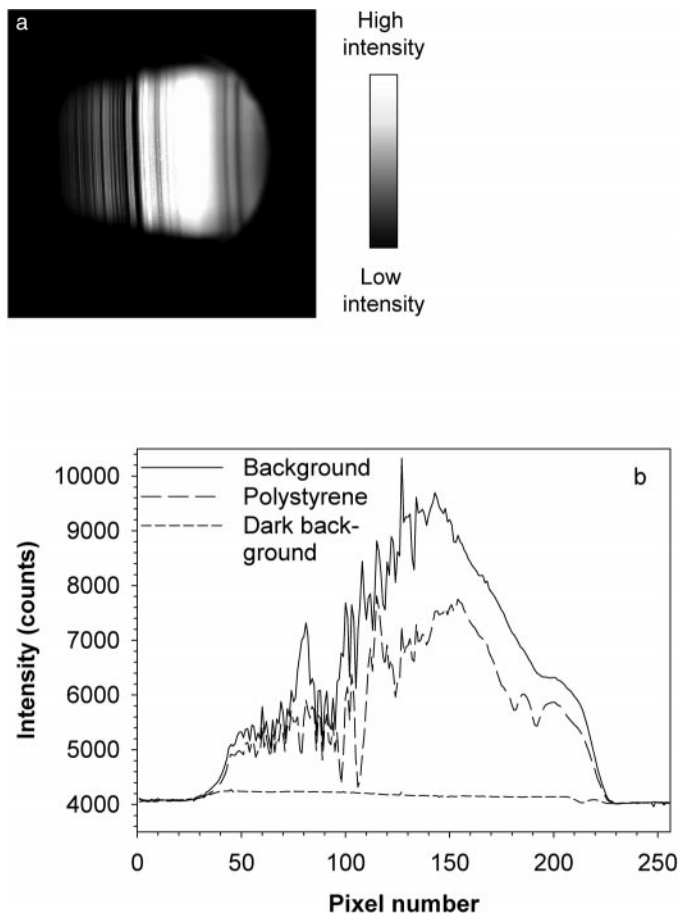
FIG. 2. (a) Spectral image obtained from a polystyrene sample. Dark bands correspond to spectral absorption features. (b) PA-IR single beam spectra.

noise was determined on a 50 pixel range corresponding to the 1150–1350 cm⁻¹ region using Omnic 6.0 (Thermo Nicolet, Madison, WI). It was determined that the frame rate does not have a significant influence on the noise level. As in the case of imaging FT-IR spectrometers using an FPA, image coaddition leads to a better noise improvement than direct frame coaddition.[14,19] In the present case, the FPA software (WinIR3) averages sequential frames with a 16-bit computer word length and is thus limited to ±1 intensity count noise. This limit was reached after coaddition of about 25 frames, which precludes further improvement using the WinIR3 software. Twenty-five-frame images were thus acquired and externally averaged for larger frame coadditions.

Fourier Transform Infrared Spectra. FT-IR spectra of the 50 μm PS standard film were collected at 4, 8, 16, and 32 cm⁻¹ resolution without zero-filling with a Nexus 670 FT-IR (Thermo Nicolet, Madison, WI) equipped with a DTGS detector. Measurements of 100% noise spectra were performed with a Magna 760 FTIR (Thermo Nicolet, Madison, WI) equipped with a liquid nitrogen-cooled mercury cadmium telluride (MCT) detector at 8 cm⁻¹ resolution without zero-filling. The peak-to-peak noise level was determined in the 1150–1350 cm⁻¹ region.

Liquid Crystal Reorientation. Electrooptically switchable liquid crystalline samples were prepared by sandwiching 4-n-pentyl-4′-cyanobiphenyl (5CB) between germanium plates following a method previously described in the literature.[20] The sample was in the nematic phase at room-temperature. The sample thickness was maintained at 15 μm using glass rod spacers. Poly(vinyl alcohol) alignment layers were deposited onto Ge plates by solvent casting and were then rubbed to introduce an in-plane preferential orientation. An electrode was attached to one edge of each plate using conductive silver paint. The electric field perturbation was applied to the sample using an arbitrary waveform generator (Stanford Research Systems model DS345, Sunnyvale, CA), which consisted of a single 100 ms pulse of a 10 V peak-to-peak, 1000 Hz sine wave. Time-resolved PA-IR spectra were acquired as a series of single frame (no coaddition) spectra at a frame rate of 115 Hz.

RESULTS AND DISCUSSION

Planar Array Infrared Spectra. Figure 2a shows the spectral image obtained when a 50 μm PS film is introduced into the optical path of the PA-IR. As the diffraction grating disperses the infrared light along the horizontal axis of the FPA, a pixel row in the spectral image corresponds to a single beam spectrum of the sample (intensity vs. pixel number/wavelength). On the other hand, pixel columns correspond to a series of spatially resolved elements along the height of the slit for a given diffracted wavelength. The top pixel rows of the spectral image are thus characteristic of the spectrum on the upper part of the sample, while those at the bottom correspond to the spectra of the lower portion of the sample. Since the height of the spectral image is ~140 pixels, 140 individual spectra can, in principle, be measured simultaneously. It is thus possible to characterize the heterogeneity of a single sample or acquire spectra from multiple samples simultaneously with a one-dimensional spatial resolution on the order of ~150 μm/pixel. Other uses of this feature of PA-IR for pixel binning and multi-beam experiments will be explored below. The spectral image in Fig. 2a is presented on a transmitted light intensity scale, so spectral absorbance features of the sample appear as dark vertical bands on a bright background.

A single beam spectrum of PS obtained from a single pixel row of Fig. 2a is shown in Fig. 2b, along with spectra of the background (open path) and dark background (blocked path) measured sequentially under the same experimental conditions. Several absorption bands can be observed for the PS sample. For instance, the strong band at pixel #105 corresponds to the 1452 cm⁻¹ band, while that at pixel #191 is due to the 1154 cm⁻¹ band. Comparison with an FT-IR spectrum of PS shows that the spectral image covers a broad range from about 1830 to 1120 cm⁻¹. It should be stressed that PA-IR is a no-moving-part spectrograph, which means that this spectral range was accessible without rotation of the diffraction grating or motion of any other component. The accessible spectral range of this instrument covers the 2000 to 975 cm⁻¹ region and is restricted by the grating efficiency function, the compound lens transmission curve, and the response cutoff of the photovoltaic MCT detectors in the FPA. The use of different gratings and lenses should make possible the recording of spectra up
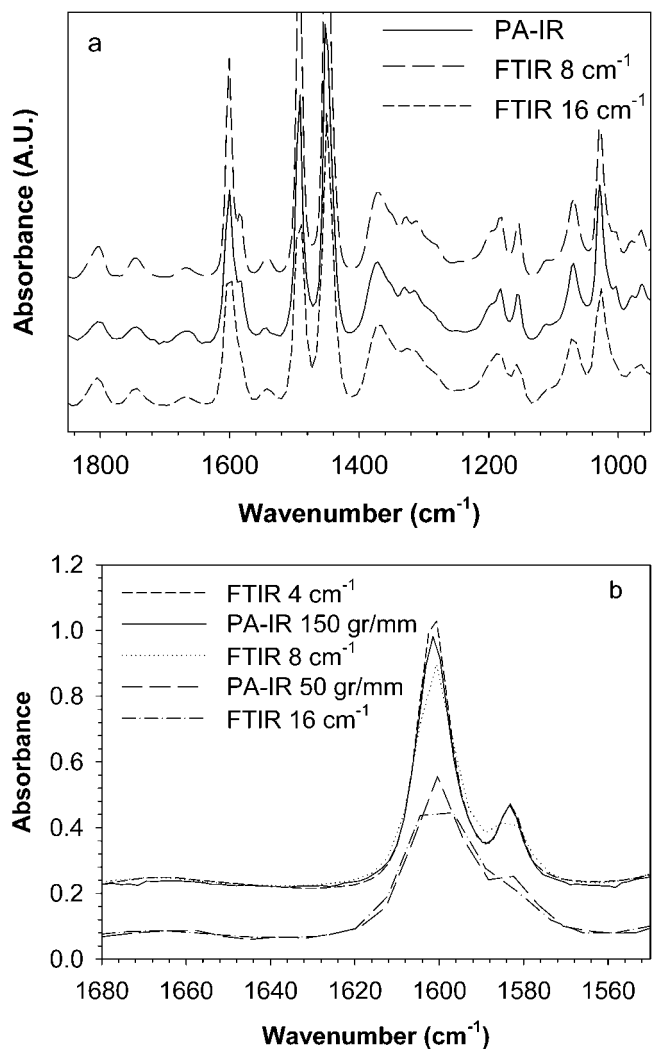
FIG. 3. (a) Polystyrene spectra obtained by PA-IR with a 50 grooves/mm grating and by FT-IR with 8 and 16 cm⁻¹ resolution. (b) Polystyrene spectra obtained by PA-IR with 50 and 150 grooves/mm gratings and by FT-IR with 4, 8, and 16 cm⁻¹ resolution.

to 4000 cm⁻¹, while the replacement of the MCT FPA with a microbolometer camera could extend the low wavenumber range to below 800 cm⁻¹, albeit at the expense of a reduced frame rate and signal-to-noise ratio.

It is clear from Fig. 2a that the actual useful image does not encompass the total 256 × 256 pixels of the FPA but is restricted to a size approximately 190 pixels wide and 140 pixels high, mainly because of the $f/\#$ of the collection optics. It should be possible to expand the spectral range by using appropriate optics. Strong water vapor absorptions also appear in both the background and sample spectra because the instrument was not purged. Future refinements will introduce a nitrogen purging system for this PA-IR spectrograph.

The absorbance spectrum of PS has been calculated using Eq. 1 and is compared in Fig. 3a with FT-IR spectra obtained at 8 and 16 cm⁻¹ resolution. This extended PA-IR spectrum was obtained by combining two separate measurements with the grating set to measure at high and low wavenumbers. The overlap between the two spectra near 1280 cm⁻¹ is barely visible. The PA-IR spectrum

has been converted from a pixel to a wavenumber scale using the calibration procedure described in the Experimental section. A good agreement is obtained between the band positions in the PA-IR and FT-IR spectra, with a deviation below 0.1 cm⁻¹, confirming the validity of this procedure. Comparison of the absorbance and shape of the bands allows an estimation of the resolution of the PA-IR spectrum recorded using a 50 grooves/mm grating to be ~14 cm⁻¹ at 1600 cm⁻¹, and ~7 cm⁻¹ at 1000 cm⁻¹. This variation of resolution as a function of wavenumber is explained by the fact that the grating disperses the infrared light in a manner such that it provides an approximately constant resolution in wavelength and not in frequency as FT-IR spectrometers do.

Figure 3b compares the spectra obtained in the 1600 cm⁻¹ region using PA-IR with 50 and 150 grooves/mm gratings with those recorded by FT-IR at 4, 8, and 16 cm⁻¹ resolution. It is clear that the use of a higher density grating increases the band absorbance and improves the resolution of the 1583 cm⁻¹ band. The spectral resolution using the second grating can be estimated to be ~5.5 cm⁻¹ over this spectral region, and the useful spectral range is ~250 cm⁻¹. Unfortunately, the grating diffraction efficiency function does not allow measurements at 1000 cm⁻¹. In contrast to FT-IR spectrometers, spectral range and resolution are not independent for a PA-IR spectrograph because the number of pixels (spectral elements) on the camera is fixed. A resolution increase by a factor of two will necessarily be obtained at the expense of a reduction of the spectral range by the same factor. Depending on the requirements of the application, it is thus possible to record PA-IR spectra with either a larger bandwidth or higher resolution, but not both simultaneously.

Evaluation of Signal-to-Noise Ratio for the Planar Array Infrared Spectrograph. In order to evaluate the sensitivity and performance of the PA-IR spectrograph in the fingerprint region, the peak-to-peak absorbance noise level was determined from a series of 100% noise spectra recorded by coadding from 1 to 1000 frames as described in the Experimental section. Figure 4 shows, on a logarithm scale, the peak-to-peak noise calculated using a single pixel row of the spectral image, as well as the noise level obtained on a conventional FT-IR equipped with an MCT detector at 8 cm⁻¹ resolution. The peak-to-peak noise is only 1.8×10^{-3} A.U. for a single frame acquisition, which clearly demonstrates that the PA-IR spectrograph possesses sufficient sensitivity to perform dynamic studies by collecting a single frame with a time resolution of 8.7 ms. This value is similar to the noise level of 2.7×10^{-3} A.U. reported by Elmore et al. using an InSb focal plane array in the C–H stretching region.[18]

Increasing the number of averaged frames leads to a significant improvement of the noise level. For example, a value of 2.0×10^{-4} A.U. was obtained by averaging 100 frames, for an acquisition time of less than a second (870 ms) and a total integration time of 7.1 ms. Since infrared spectrometers are usually detector-noise limited, a square root reduction of the noise as a function of integration time (number of frames or scans) is expected.[1] In general agreement with this, Fig. 4 shows that the evolution of the base 10 logarithm of the noise as a function of acquisition time is described by a straight line

with a slope of -0.43 for PA-IR data, while the curve for the noise level measured using a conventional FT-IR does indeed follow the expected square root dependency. Close observation suggests that the PA-IR noise values for a small number of frames also follow the square root behavior. The slight departure for larger acquisition time is probably due to a drift of the FPA response. A better control of the instrument environment might lead to enhanced long-term stability and thus to improved noise levels and sensitivity.

It can be observed in Fig. 4 that the noise level determined using an FT-IR spectrometer is slightly lower than that obtained by PA-IR when considering a single pixel row. This is of course only applicable in their region of overlap for relatively long acquisition times, i.e., above 500 ms. This result is not surprising considering the fundamental characteristics of the single element and FPA detectors. It is, however, possible to improve the signal-to-noise ratio obtained in a PA-IR experiment by averaging several vertical pixel rows from the same frame.

Averaging 100 pixel rows significantly decreases the noise values, by a factor of up to 7, and allows PA-IR to present equivalent or even better noise levels than a conventional FT-IR instrument for a similar acquisition time. It should nevertheless be acknowledged that for long acquisition times, the actual performance of the PA-IR spectrograph does not yet match that of a research-grade FT-IR instrument. The noise improvement does not follow the square root dependency, possibly because of an inhomogeneity of the light intensity across the height of the FPA. Pixel binning can lead to a peak-to-peak noise as low as 2.4×10^{-4} A.U. for a single frame acquisition that can be reproduced continuously every 8.7 ms. This procedure should thus prove useful for raising the sensitivity for real-time dynamic studies and for the determination of weak spectral features of homogeneous samples, such as the continuous detection of a dilute gas.

Time-Resolved Study of Liquid Crystal Reorientation. The reorientation of liquid crystalline samples under an external electric field has attracted much attention.[20–28] In spite of a large amount of published work, it has not yet been clearly established whether the rigid and flexible moieties of the liquid crystal follow the same dynamics. The effect of the polymeric alignment layer on the reorientation dynamics of the liquid crystal is also of scientific and technological interest.[20,23] Time-resolved infrared spectroscopy has proven to be the tool of choice to study such systems, but conventional approaches suffer from the limitations pointed out earlier. The purpose of the following experiment was to evaluate the ability of PA-IR to contribute to the understanding of the dynamics of liquid crystal reorientation in particular, and, in general, to the real-time study of dynamic phenomena. Since the perturbation induced in the 5CB sample was brought about by the application of a single electric field pulse and not by a cyclic series of pulses, this study demonstrates the applicability and performance of PA-IR to the study of truly irreversible phenomena.

In the following measurements, two different spatial locations of the FPA have been used to simultaneously measure spectra with the infrared beam polarized parallel (*p*) and perpendicular (*s*) to the rubbing direction of the poly(vinyl alcohol) alignment layer. As shown in Fig. 5a,
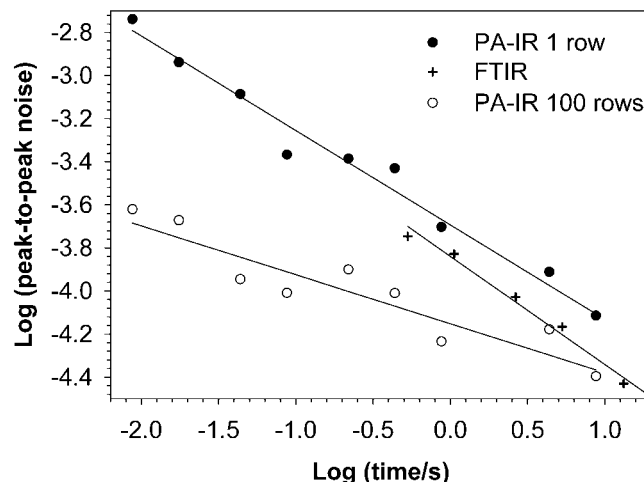

FIG. 4. Evolution of the peak-to-peak noise level in the 100% noise spectra as a function of acquisition time using the PA-IR spectrograph and a research-grade FT-IR spectrometer. Empty symbols show the effect of binning up to 100 pixel rows in the PA-IR spectral image with a constant acquisition time.

approximately 35 and 50 useful pixel rows were available in the *p* (top) and *s* (bottom) regions of the images, respectively. Figure 5b shows the infrared spectra obtained for both polarizations before application of the electric field pulse (off) and while the field was on (on). Because of the absence of a purged environment, small water vapor bands were present in the spectra, but they did not affect the time-resolved results since they were constant throughout the 1 s experiment.

Clear differences are observable between the *p*- and *s*-polarized spectra before the perturbation (off). The 1606 and 1494 cm^{-1} bands, attributed to aromatic C–C stretchings of the rigid moiety,[27] are much more intense with *p*-polarization, indicating a large planar orientation along the rubbing direction of the alignment layer. Indeed, an orientation function[29] of 0.47 can be calculated from the 1606 cm^{-1} band, assuming that the orientation is uniaxial and that the transition moment of the band makes a 16° angle with the chain axis.[27] A perfect orientation would have yielded a maximum value of the orientation function equal to 1.

Upon application of the electric field, major changes appear in the *p*-polarized spectrum, the most evident being the reduction in absorbance of the intense C–C stretching bands (1606 and 1494 cm^{-1}). This was expected since it is well known that nematic liquid crystals with positive dielectric anisotropy such as 5CB orient with their molecular long axis along the electric field direction.[21] A large reduction of the absorption for the bands parallel to the chain axis occurs since their transition moments now become parallel to the propagation direction of the infrared beam and there is no coupling between the polarized electric field and the transition dipoles. In contrast, no significant variation appears, within experimental error, in the *s*-polarized spectra because the contribution of the transition moments perpendicular to the long axis is not influenced by the rotation of the molecules as long as a cylindrical symmetry is preserved. When the field is removed, the molecules reorient back to their initial state parallel to the alignment layer, and
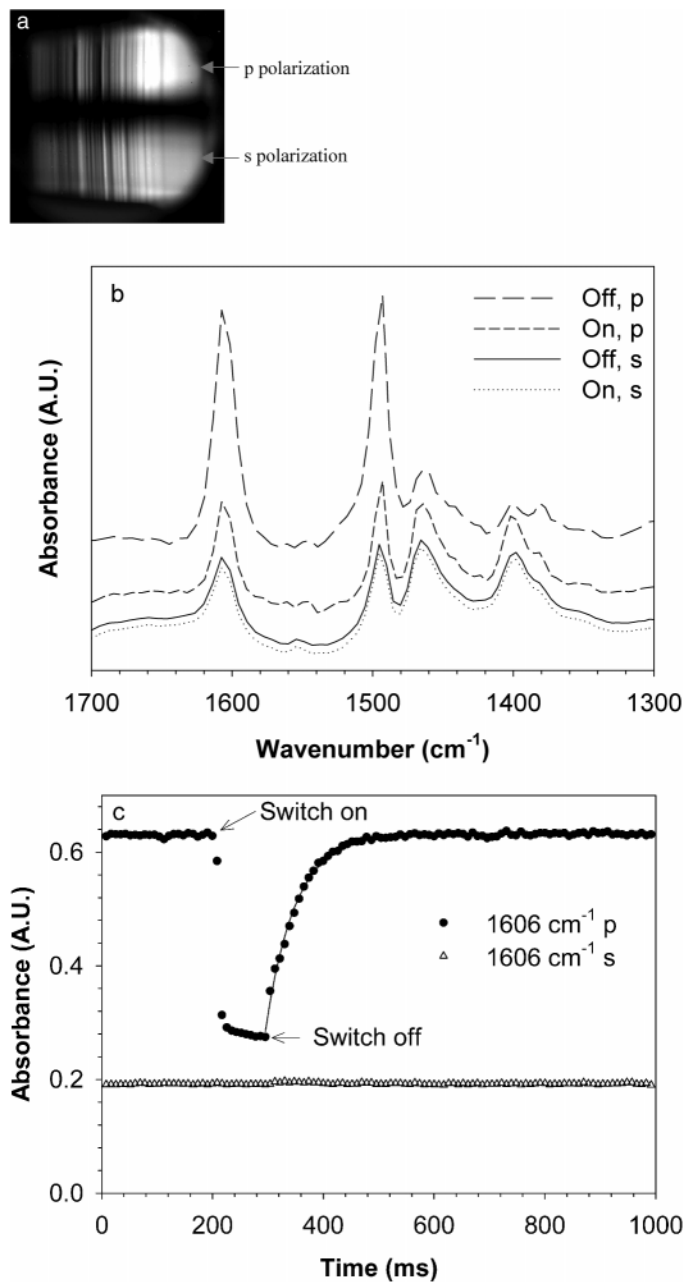
FIG. 5. (**a**) PA-IR spectral image showing the use of multiple beam measurements. The top and bottom images are *p*- and *s*-polarized, respectively, before application of the electric field. (**b**) Infrared spectra of the 5CB liquid crystal obtained with *p*- and *s*-polarizations before (off) and during (on) the 100 ms electric field pulse. (**c**) Kinetics of orientation obtained with *p*- and *s*-polarizations for a 5CB liquid crystalline sample submitted to a single 100 ms electric field pulse. The continuous curve is a fit of the reorientation kinetics using a single exponential function.

the spectra are identical to those obtained before application of the perturbation.

Figure 5c shows the time-resolved absorbance changes for the 1606 cm^{-1} band for both polarizations before, during, and after application of the 100 ms electric field pulse. The data were acquired in a 1-second-long experiment by binning over 30 pixel rows. In the *p*-polarized spectra, the application after 200 ms of the electric field is evident from the abrupt decrease in absorbance. Ori-

entation of the liquid crystals develops almost instantaneously within the time resolution of 8.7 ms available with the actual setup. It is nevertheless possible to observe that a slower process continues increasing the orientation during the following ~80 ms.

The PA-IR spectrograph can easily resolve the reorientation process when the electric field is turned off, with very low scatter in the data. The relaxation curve was fitted using a single exponential function, as shown by the continuous curve, which yielded a relaxation time of 55 ms. This value is about two times larger than that previously published for a similar system.[20] This difference is due to a change in the effective anchoring strength of the alignment layer caused by the presence of micro grooves induced during rubbing.

As mentioned above, no significant change occurs in the *s*-polarized spectra. It is nevertheless interesting to observe the very low scatter in the data of Fig. 5c, the dispersion being less than 0.005 absorbance units around the mean value. These results demonstrate that PA-IR should allow the observation of weak absorbance variations for time-resolved phenomena with an 8.7 ms time resolution. It should be stressed that total measurement time to determine both the *p* and *s* spectra was only 1 s and that a single perturbation was applied, showing that the study of irreversible phenomena on this time scale will be possible using PA-IR.

Even for the study of reversible phenomena such as the liquid crystal reorientation, the short time required by PA-IR to characterize the whole dynamic process can make this approach attractive over conventional step-scan FT-IR. Indeed, in order to measure a single interferogram at a resolution of 8 cm^{-1} over a spectral range extending from 500 to 2000 cm^{-1} using a step-scan FT-IR, time-resolved data must be acquired at 512 steps of the moving mirror. According to the data of Fig. 5c, a repetition rate of 3 Hz for the successive electric field pulses should not be exceeded in order to allow sufficient relaxation time for the sample to relax to its initial state. Faster repetition rates would yield incorrect and misleading data, a danger always present when using cyclic measurement schemes. This leads to an acquisition time of 171 s to obtain a single scan using step-scan FT-IR, more than two orders of magnitude slower than PA-IR. Additional scans may be necessary to obtain a sufficient signal-to-noise ratio, increasing the total acquisition time significantly. Although such a reduced experiment time is an achievement in itself, the main advantage of PA-IR resides in the decreased risk of sample or instrumental fluctuations during the measurements, thus diminishing the possibility of introducing artifacts in the time-resolved data.

The performance of the PA-IR spectrograph can also be compared with that of ultra-rapid-scanning FT-IR. The prototype developed by Griffiths et al.[2] can actually provide a slightly faster frame rate than the PA-IR spectrograph used in this study, in addition to the obvious advantage of recording a complete infrared spectrum as compared to a bandwidth on the order of 600–700 cm^{-1} for PA-IR (although future developments should extend the bandwidth for a single measurement). In comparing the maximum acquisition rate, one nevertheless must consider that artifacts can be introduced in the spectra if

sample modifications occur during the time necessary to perform the measurement. As a rule of thumb, Smith and Palmer have suggested that the time necessary to perform a scan should be an order of magnitude shorter than the half life of the dynamic event being examined.[4] We have to emphasize that although the frame rate used in this study using PA-IR was 115 Hz, the actual data acquisition was performed as a series of 71 µs snapshots. From that standpoint, this was more than an order of magnitude faster than the most rapid scan time using FT-IR. In any case, sample changes during the integration time would generate an averaged spectrum in a PA-IR experiment, and not spectral artifacts as in an FT-IR measurement, since the interferogram would have been altered by the sample changes. The possibility of pixel binning also provides a noise level advantage to PA-IR as compared to ultra-rapid-scanning FT-IR. The possibility of simultaneously recording p and s spectra is also a fundamental advantage of the use of a focal plane array detector.

Despite its longer measurement time, step-scan FT-IR distinguishes itself from PA-IR in its actual form and from URS-FT-IR in the possibility of acquiring time-resolved spectra in the micro- and nanosecond range. For example, step-scan FT-IR can follow the orientation process of liquid crystals when the electric field is switched on.[22–25] It can reasonably be expected that technological improvements will lead to faster and larger infrared FPAs that will increase the time resolution without the need to sacrifice spectral range, thereby limiting the time resolution advantage of step-scan FT-IR to experiments requiring sub-100 µs resolution. Smaller commercially available FPAs already provide much higher frame rates than the 256×256 FPA used in this study. For instance, 128×128 MCT FPAs can already generate full images at a frame rate of 1600 Hz, meaning that a time resolution of 625 µs can readily be achieved if one can afford a reduced spectral range or resolution. InSb arrays with 128×128 pixels can also be used at frame rates larger than 15 000 Hz, but are restricted to the frequencies above 2000 cm^{-1}. In a recently published paper, Snively et al. have used a 64×64 MCT FPA using a ''rolling'' rather than a ''snapshot'' mode to probe the reorientation dynamics of 5CB with a time resolution below 100 µs.[31] It can also be predicted that better noise levels will be obtainable for a given measurement time using faster FPAs as the duty cycle will be increased.

CONCLUSION

A planar array infrared spectrograph working between 2000 and 975 cm^{-1} has been constructed and its performance validated. The instrument allows recording single frame spectra with peak-to-peak noise levels as low as 2.4×10^{-4} A.U. This performance makes possible the real-time study of irreversible phenomena with an 8.7 ms time resolution. The spectrograph was successfully applied to study time-resolved reorientation dynamics of a 5CB liquid crystalline sample under an external electric field. A single 1 s experiment has allowed the precise determination of the relaxation time after switching off the electric field. It has also been shown that the large size of the focal plane array allows collecting simulta-

neously p- and s-polarized spectra. Future technological developments should lead to faster, larger, more stable, and cheaper FPAs, thus improving the accessibility, time-resolution, signal-to-noise ratio, and potential for multi-beam experiments of the PA-IR spectrograph.

1. P. R. Griffiths, *Chemical Infrared Fourier Transform Spectroscopy* (Wiley-Interscience, New York, 1975).
2. P. R. Griffiths, B. L. Hirsche, and C. J. Manning, Vib. Spectrosc. **19,** 165 (1999).
3. H. Wang, R. A. Palmer, and C. J. Manning, Appl. Spectrosc. **51,** 1245 (1997).
4. G. D. Smith and R. A. Palmer, ''Fast Time-Resolved Mid-Infrared Spectroscopy Using an Interferometer'', in *Handbook of Vibrational Spectroscopy,* P. R. Griffiths and J. M. Chalmers, Eds. (John Wiley and Sons, Chichester, 2002), vol. 1, p. 625.
5. A. K. Dioumaev and M. S. Braiman, J. Phys. Chem. B **101,** 1655 (1997).
6. K. Masutani, H. Sugisawa, A. Yokota, Y. Furukawa, and M. Tasumi, Appl. Spectrosc. **46,** 560 (1992).
7. S. Ekgasit, H. W. Siesler, and P. A. M. Steeman, Appl. Spectrosc. **53,** 1535 (1999).
8. K. Heyne, N. Huse, E. T. J. Nibbering, and T. Elsaesser, Chem. Phys. Lett. **382,** 19 (2003).
9. M. Towrie, D. C. Grills, J. Dyer, J. A. Weinstein, P. Matousek, R. Barton, P. D. Bailey, N. Subramaniam, W. M. Kwok, C. S. Ma, D. Phillips, A. W. Parker, and M. W. George, Appl. Spectrosc. **57,** 367 (2003).
10. C. S. Colley, D. C. Grills, N. A. Besley, S. Jockusch, P. Matousek, A. W. Parker, M. Towrie, N. J. Turro, P. M. W. Gill, and M. W. George, J. Am. Chem. Soc. **124,** 14952 (2002).
11. C. Pellerin, R. E. Prud'homme, M. Pézolet, B. A. Weinstock, and P. R. Griffiths, Macromolecules **36,** 4838 (2003).
12. C. M. Snively, S. Katzenberger, G. Oskarsdottir, and J. Lauterbach, Opt. Lett. **24,** 1841 (1999).
13. R. Bhargava, T. Ribar, and J. L. Koenig, Appl. Spectrosc. **53,** 1313 (1999).
14. R. Bhargava and I. W. Levin, Anal. Chem. **73,** 5157 (2001).
15. P. Colarusso, L. H. Kidder, I. W. Levin, J. C. Fraser, J. F. Arens, and E. N. Lewis, Appl. Spectrosc. **52,** 106A (1998).
16. K. Masutani, K. Numahata, K. Nishimura, S. Ochiai, Y. Nagasaki, N. Katayama, and Y. Ozaki, Appl. Spectrosc. **53,** 588 (1999).
17. S. M. Alawi, T. Krug, and H. H. Richardson, Appl. Spectrosc. **47,** 1626 (1993).
18. D. L. Elmore, M. W. Tsao, S. Frisk, D. B. Chase, and J. F. Rabolt, Appl. Spectrosc. **56,** 145 (2002).
19. C. M. Snively and J. L. Koenig, Appl. Spectrosc. **53,** 170 (1999).
20. C. M. Snively and J. L. Koenig, J. Mol. Struct. **521,** 121 (2000).
21. H. W. Siesler, I. Zebger, C. Kulinna, S. Okretic, S. Shilov, and U. Hoffmann, ''Segmental Mobility of Liquid Crystals and Liquid-Crystalline Polymers under External Fields: Characterization by Fourier-Transform Infrared Polarization Spectroscopy'', in *Modern Polymer Spectroscopy,* G. Zerbi, H. W. Siesler, I. Noda, M. Tasumi, and S. Krimm, Eds. (Wiley-VCH, Weinheim, 1999), p. 33.
22. A. R. Noble, H. J. Kwon, and R. G. Nuzzo, J. Am. Chem. Soc. **124,** 15020 (2002).
23. E. Klimov, M. Fuelleborn, and H. W. Siesler, Appl. Spectrosc. **57,** 499 (2003).
24. A. R. Noble-Luginbuhl, R. M. Blanchard, and R. G. Nuzzo, J. Am. Chem. Soc. **122,** 3917 (2000).
25. W. G. Jang and N. A. Clark, Phys. Rev. E **63,** 031707 (2001).
26. R. Bhargava and I. W. Levin, Appl. Spectrosc. **57,** 357 (2003).

27. A. Hatta, Mol. Cryst. Liq. Cryst. **74,** 195 (1981).
28. V. G. Gregoriou, J. L. Chao, H. Toriumi, and R. A. Palmer, Chem. Phys. Lett. **179,** 491 (1991).
29. T. Buffeteau and M. Pézolet, "Linear Dichroism in Infrared Spectroscopy", in *Handbook of Vibrational Spectroscopy,* P. R. Griffiths and J. M. Chalmers, Eds. (John Wiley and Sons, Chichester, 2002), vol. 1, p. 693.
30. D. W. Berreman, Phys. Rev. Lett. **28,** 1683 (1972).
31. C. M. Snively, C. Pellerin, J. F. Rabolt, and D. B. Chase, Anal. Chem. **76,** 1811 (2004).